Phase equilibria in the liquid sulphur-tellurium system: structural changes and two-melt phase separation

1992 J. Phys.: Condens. Matter 4 4335

(http://iopscience.iop.org/0953-8984/4/18/002)

J. Phys.: Condens. Matter 4 (1992) 4335–4349. Printed in the UK

Phase equilibria in the liquid sulphur–tellurium system: structural changes and two-melt phase separation

Y Tsuchiya
Department of Physics, Faculty of Science, Niigata University, 2-8050 Ikarashi, Niigata 950-21, Japan

Received 23 December 1991

Abstract. A two-melt region bounded by a closed loop in the composition–temperature plane has been found in the liquid S–Te system, which is the first example for a liquid having electrical conductivity. It is located in an extremely narrow range centred at about 39.2 at.% S and 715 °C near the threshold of the non-metal–metal transition. It has been shown that structural change in the liquid causes the two-melt phase separation.

1. Introduction

Liquid Te transforms to a low-temperature form (hereafter referred to as the L form) at supercooled temperatures. The structure of the L form is characterized by twofold coordination similar to that in liquid Se. Above the melting temperature (451 °C) the change is almost complete and liquid Te is essentially in a different form (the H form), the co-ordination number of which is about three (Mennele *et al* 1988, 1989). The structural change proceeds quite rapidly at around 353 °C, where the specific heat has a marked peak (Tsuchiya 1991a). The L form of Te is stabilized by adding Se, which is manifested by the fact that the extrema in the thermal expansion coefficient (Thurn and Ruska 1976), the isothermal compressibility (Takimoto and Endo 1982, Tsuchiya 1991b), and the specific heat (Kakinuma and Ohno 1987) shift to the higher temperatures with increasing Se composition. Analysis of the heat of mixing (Tsuchiya 1986a) and the specific heat measurements (Kakinuma and Ohno 1988) indicate that S stabilizes the L form of Te as well.

In a series of papers, the present author and Seymour have developed a model referred to as an inhomogeneous structure model (IHSM) to describe the temperature variation of thermodynamic parameters associated with structural changes in liquid Se–Te (Tsuchiya and Seymour 1982, 1985). The transition can be described satisfactorily by a single parameter, the dependence of which on temperature and pressure obeys a kind of mass-action law. It is, therefore, of interest to see whether or not such a model can be applied to the other system.

In this paper, the molar volume of the liquid S–Te system has been investigated using a high energy γ-ray attenuation method. The overall temperature and composition dependence of the volume is found to be much the same as that reported for the liquid Se–Te system. The results, therefore, indicate that structural changes similar to those

0953-8984/92/184335 + 15 $04.50

in the liquid Se–Te alloy take place. In addition, as preliminary results have been reported (Tsuchiya 1989), the two-melt phase appears in a quite narrow region having a closed boundary in the composition–temperature plane well above the equilibrium liquidus temperature. In this paper, the phase boundary has been determined in more detail and the unusual phase separation has been investigated based on the IHSM. It has been shown that instability of the alloy is a consequence of the L- to H-form transition in the liquid.

2. Experiment

The molar volume has been deduced from the linear attenuation coefficient of high-energy (661.6 keV) γ-rays from ^{137}Cs. Since the details of the experimental procedure were the same as those reported elsewhere (Tsuchiya 1988), only essential points are described in the following. The mass absorption coefficients of S and Te were determined using a powder specimen compressed into a steel tube. They were respectively 0.07667 ± 0.00007 and $0.07182 \pm 0.00005\ cm^2\ g^{-1}$. An ampoule was made of fused silica. Two polished discs were fused to the ends of a tube to form an ampoule. The path length of the ampoule was determined by measuring the linear absorption coefficient of mercury in the ampoule and comparing this with that in a standard cell made of fused silica. A typical cell was 2–2.5 cm long and 1.1 cm in inner diameter.

To investigate the existence of a meniscus, which should appear in a liquid in the two-melt phase, a specimen sealed in a fused silica tube with inner diameter 1.3 cm was used. The effective path length of a specimen was determined using the method described above. The cell was set vertically on a fused silica holder which could be moved up and down with respect to a γ-ray beam as shown schematically in figure 1.

The temperature was controlled by a digital temperature controller which could maintain a temperature within ± 0.5 °C. The vertical temperature gradient was less than 1 °C for the volume measurements and about 2 °C over a specimen 3 cm long for the meniscus investigation.

Measurements were started after shaking a specimen kept at high temperature to ensure complete mixing. More than 4×10^6 counts were accumulated to make the counting statistics less than 5×10^{-4} for the volume measurements and about 3×10^5 counts were collected for investigating the meniscus. The whole system was controlled by a computer, including correction due to gain drift during measurements. The uncertainty of the volume was estimated to be within $\pm 0.3\%$.

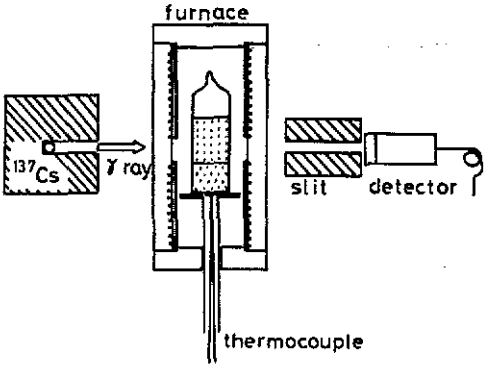

Figure 1. Schematic drawing of the experimental set-up. The slit consists of two Pb blocks 5 cm thick aligned 5 cm apart through which a bore 0.6 cm in diameter was drilled.

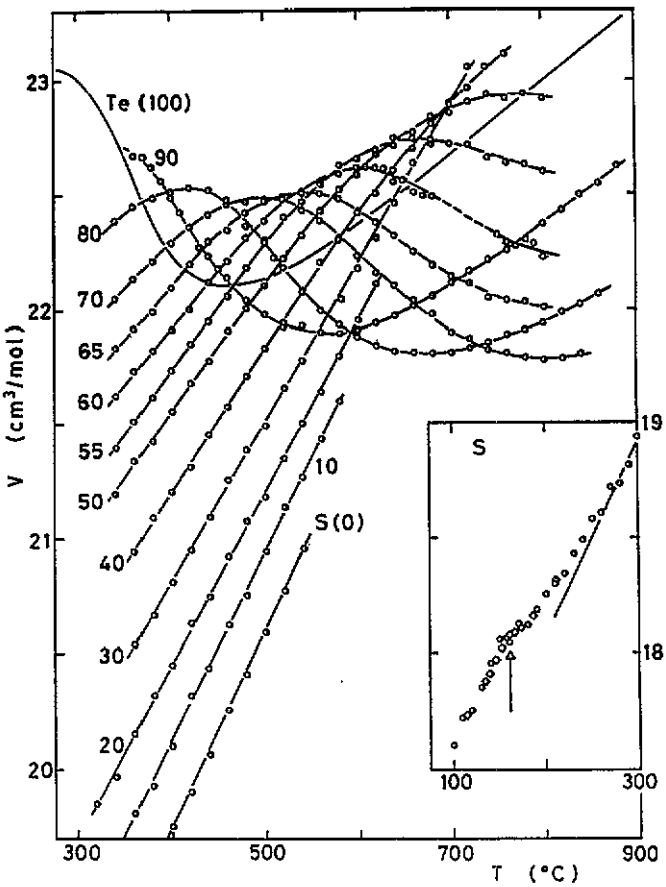

Figure 2. Molar volume (V) for the liquid S–Te system as a function of temperature. Curves are those obtained by fitting the data to equation (3) except for three S-side alloys and S where a linear temperature dependence has been assumed. The dotted portion for 60 at.% Te is the two-melt region. The curve for Te is from Tsuchiya (1991a). Numbers on the data indicate atomic per cent of Te. The inset shows the data for S around the polymerization point (159 °C: an arrow). The reference data (diamonds) are from Kellas (1918) and the solid line is an extrapolation of that shown in the main plot.

3. Results

Figure 2 shows the molar volume, V, of the liquid S–Te system as a function of temperature, T, and the numerical data are listed in table 1. The results for S are in reasonable agreement with those reported previously in the overlapping temperature region, as shown in the inset of the figure (Kellas 1918). A minimum in the V–T curve for Te shifts towards higher temperatures with increasing S fraction and a local maximum appears at the lower temperature. Except for the intermediate temperature range, where the volume contracts with increasing temperature, the volume increases almost linearly, as is usually observed for liquid metals. The same type of V–T curve has been observed for the liquid Se–Te system (Thurn and Ruska 1976, Tsuchiya 1988). For S and an alloy containing more than 60 at.% s, only the low-temperature portion of the whole V–T

Table 1. Molar volume of the liquid S–Te system ($cm^3\,mol^{-1}$). The data for Te are taken from a previous report (Tsuchiya 1991a).

T (°C)	S_{100}	$S_{90}Te_{10}$	$S_{80}Te_{20}$	$S_{70}Te_{30}$	$S_{60}Te_{40}$	$S_{50}Te_{50}$	$S_{45}Te_{55}$
100	17.61						
110	17.72						
120	17.75						
130	17.86						
140	17.96						
150	18.06						
160	18.05						
170	18.13						
180	18.13						
190	18.19						
200	18.26						
210	18.31						
220	18.35						
230	18.43						
240	18.49						
250	18.59						
260	18.61						
270	18.72						
280	18.74	19.16					
290	18.81						
300	18.95	19.30					
320	19.08	19.47	19.86				
340	19.28	19.63	19.96			21.19	21.38
360	19.42	19.82	20.16	20.54	20.95	21.34	21.52
380	19.55	19.92	20.33	20.67	21.10	21.42	21.61
400	19.75	20.14	20.45	20.81	21.20	21.56	21.73
420	19.90	20.29	20.65	20.95	21.31	21.70	21.85
440	20.06	20.44	20.71	21.09	21.45	21.77	21.96
460	20.27	20.61	20.93	21.26	21.58	21.92	22.06
480	20.38	20.75	21.01	21.43	21.71	22.02	21.19
500	20.60	20.95	21.18	21.49	21.84	22.11	22.31
520	20.78	21.10	21.35	21.67	21.94	22.22	22.40
540	20.96	21.27	21.51	21.79	22.09	22.33	22.47
560		21.44	21.64	21.90	22.21	22.42	22.54
580		21.60	21.80	21.05	22.31	22.52	22.63
600			21.96	22.18	22.43	22.59	22.61
620			22.12	22.30	22.50	22.70	22.69
640			22.40	22.46	22.60	22.75	22.71
660				22.64	22.70	22.77	22.75
680				22.71	22.81	22.81	22.74
700				22.89	22.90	22.85	22.73
720				23.06	22.96	22.90	21.72
740					23.06	22.94	22.67
760					23.11	22.91	22.64
780						22.94	22.63
800						22.91	22.59

Table 1 *continued*

T (°C)	$S_{40}Te_{60}$	$S_{35}Te_{65}$	$S_{30}Te_{70}$	$S_{20}Te_{80}$	$S_{10}Te_{90}$	Te_{100}
280						23.03
290						23.02
300						23.00
310						22.97
320						22.92
330						22.85
340	21.63	21.84	22.05	22.39		22.77
350						22.67
360	21.74	21.92	22.14	22.45	22.67	22.56
370					22.67	22.47
380	21.82	21.99	22.21	22.48	22.62	22.39
390					22.56	22.32
400	21.91	22.10	22.29	22.51	22.49	22.26
410					22.42	22.21
420	22.03	22.20	22.36	22.53	22.35	22.18
430					22.27	22.15
440	22.12	22.30	22.41	22.52	22.24	22.13
450					22.18	22.12
460	22.21	22.35	22.46	22.48	22.15	22.12
470						22.11
480	22.30	22.42	22.46	22.37	22.05	22.12
490						22.12
500	22.38	22.48	22.48	22.28	21.98	22.14
510						22.14
520	22.48	22.48	22.48	22.19	21.92	22.17
540	22.50	22.52	22.43	22.09	21.94	22.22
560	22.55	22.50	22.38	21.99	21.90	22.28
580	22.59	22.48	22.31	21.94	21.90	22.32
600	22.62	22.42	22.23	22.88	21.91	22.37
620	22.62	22.38	22.16	21.84	21.94	22.43
640	22.55	22.33	22.11	21.82	21.98	22.48
660	22.50	22.25	22.04	21.81	22.04	22.56
680	22.50	22.19	21.98	21.81	22.06	22.62
700	—	22.14	21.91	21.81	22.11	22.68
720	—	22.11	21.88	21.83	22.17	22.75
740	—	22.05	21.82	21.85	22.22	22.78
760	22.28	22.05	21.81	21.88	22.26	22.85
780	22.29	22.04	21.79	21.91	22.31	22.91
800	22.23	22.01	21.78	21.95	22.37	23.02
820		21.99	21.78	21.99	22.43	23.05
840			21.81	22.02	22.50	23.10
860				22.07	22.55	23.17
880					22.63	23.24

curve can be observed and the volume increases almost linearly with temperature, although it is inferred from the results for Te-rich alloys that the volume contraction would also take place for S-rich alloys at a much higher temperature.

The isotherms of V at several temperatures are plotted in figure 3. At low temperatures the volume increases almost linearly with Te composition while it irregularly decreases at the Te-rich side towards the Te value. A local maximum in the isotherm shifts to the S-rich side as the temperature rises, and the volume changes linearly at the Te-rich side as well, irrespective of the anomalous contraction in the moderate composition range.

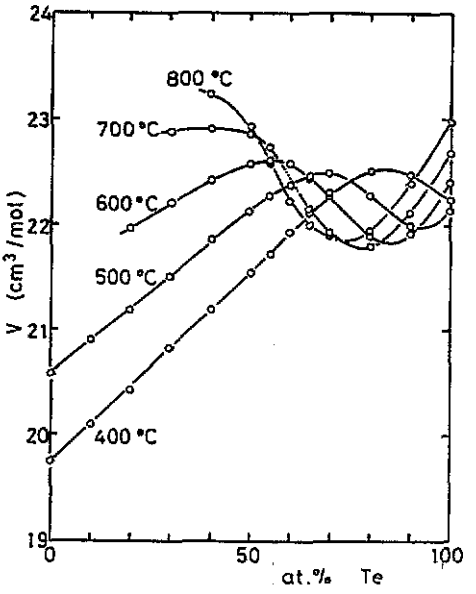

Figure 3. Molar volume (V) for the S–Te system as a function of Te composition at several temperatures. The dotted portion at 700 °C represents the two-melt region.

To calculate the thermal expansion coefficient, $\alpha_P = 1/V(\partial V/\partial T)_P$, the V–T curves for alloys with more than 40 at.% Te have been fitted to equation (3) in the following section. The results are shown by the smooth curves joining the data in figure 2. For S-rich alloys, the data have been fitted to a linear temperature dependence. The thermal expansion coefficient calculated in this way is plotted in figure 4.

While the overall dependence on temperature and composition of the volume is quite similar to that found for the Se–Te system, a clear anomalous break was found in the V–T curve of $S_{40}Te_{60}$ as reproduced in the inset of figure 5 (hereafter numerical suffices refer to atomic per cent of the constituents). The results suggest that marked increase of the attenuation of γ-rays takes place in $S_{40}Te_{60}$ between 700 and 740 °C. Preferential evaporation of S into an open volume in the specimen ampoule could bring about an increase of γ-ray attenuation, which may, however, be ruled out, because it is not easy to explain thus the recovery of the volume above 750 °C to the values extrapolated from low temperatures.

Vertical scanning of γ-ray counting using a cylindrical specimen of $S_{40}Te_{60}$ about 3 cm long was then carried out using the experimental set-up shown schematically in figure 1. The results are plotted in figure 5. Figure 5 shows γ-ray counts as a function of vertical position of the specimen with respect to the γ-ray beam at three temperatures

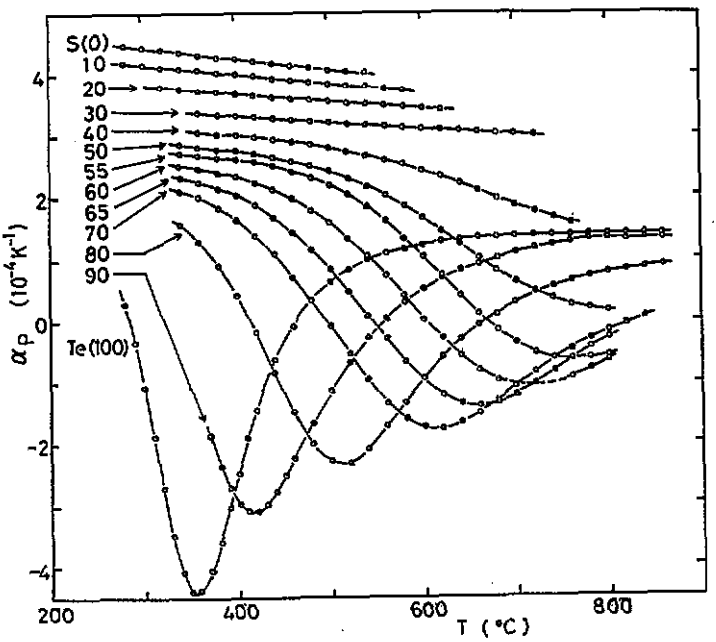

Figure 4. Thermal expansion coefficient (α_P) for the S–Te system. Numbers on the data indicate atomic per cent of Te.

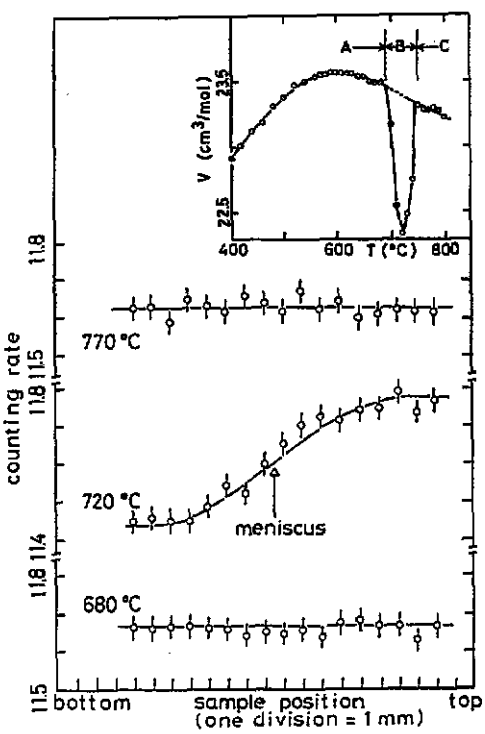

Figure 5. Search for a meniscus in $S_{40}Te_{60}$: γ-ray counts as a function of specimen position. An arrow shows the position of the meniscus due to phase separation. The inset shows the V–T curve for $S_{40}Te_{60}$. The data in the two-melt region are apparent values.

covering the range B indicated in the inset, where unusual increase of γ-ray attenuation is observed. In the regions A and C, the γ-ray counts are constant over the specimen, while in the region B the attenuation was found to be larger at the bottom of the specimen. The curve in the figure is a calculated counts versus position curve assuming that the alloy has a meniscus due to phase separation, where the effects due to finite slit width have been taken into account. It may be concluded from these experiments that an unusual phase separation, which has a lower critical solution temperature (LCST) and an upper critical solution temperature (UCST), takes place.

The compositions of the respective liquids were graphically determined using the following relation,

$$(1/d)\ln(N/N_0) = -(1/V)[x\mu_S A_S + (1-x)\mu_{Te}A_{Te}] \qquad (1)$$

where N and N_0 are γ-ray counts through the ampoule with and without specimen, respectively, d the specimen thickness, μ_i the mass absorption coefficient and A_i the atomic mass, i is S or Te. The right-hand side may be evaluated using the isotherms of V in figure 3. In the two-melt region, the composition x in the liquid portion seen by a

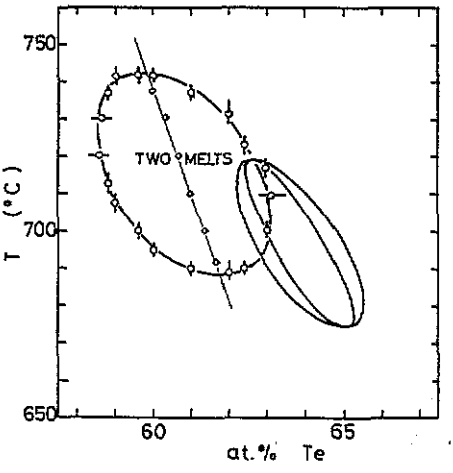

Figure 6. The two-melt region for the S–Te system. Circlets show the boundary and diamonds indicates the diameters. The rugby ball is a theoretical two-melt region: the inner oval is the spinodal line given by the condition $T_c = T$ shown in figure 9, and the outer is the binodal line obtained graphically from the chemical potential as a function of composition (cf figure 10).

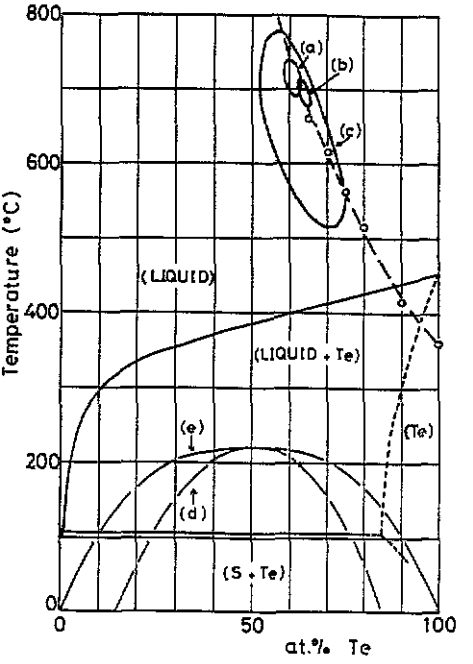

Figure 7. The phase diagram for the S–Te system. An oval (a) is the experimental two-phase region shown in figure 6; (b) and (c), respectively, are theoretical calculations at 0 and 10^8 Pa (1 kbar). The equilibrium phase diagram below 500 °C is from Hansen and Anderko (1958). Circlets show the temperatures for minima in α_P and the broken curve through them is T^* given by equation (11). The two convex curves below the liquidus line are the spinodal (d) and binodal (e) lines corresponding to the phase separation caused by the intrinsic repulsive interaction, w, between S and Te.

γ-ray beam rapidly changes with temperature, which causes a clear break in the V–T curve as shown in the inset of figure 5. Then the onset of demixing was also detected by observing inflection points in the V–T curve measured at every 5 °C by changing composition by 1 at.%. The phase boundary determined in this way is plotted in figure 6 and its location in the whole composition–temperature plane is shown in figure 7. As seen in figures 6 and 7, the two-melt region is located in a quite narrow range. The diameters of the two-phase region appear to fall on a straight line. From the diagram LCST and UCST have been determined as 689 ± 5 °C at 38.0 ± 0.4 at.% S and 745 ± 5 °C at 40.4 ± 0.4 at.% S, respectively, and the centre 715 ± 5 °C at 39.2 ± 0.4 at.% S.

4. Discussion

4.1. Structural changes

It is believed that above the critical polymerization temperature (159 °C), liquid S takes a chain structure with twofold coordination (Tobolsky and MacKnight 1965), although a different structural model has recently been presented based on the pair correlation function (Winter *et al* 1990). On the other hand, neutron diffraction experiments have revealed that liquid Te transforms in the supercooled temperatures to a liquid having a structure isomorphous with that of liquid Se, characterized by twofold coordination (Mennele 1988, 1989). The structural change in supercooled liquid Te has also been confirmed by thermodynamic measurements: the specific heat, thermal expansion coefficient and sound velocity show peaked extrema around 353 °C (Tsuchiya 1991a) in accord with the thermodynamic model previously proposed based on the data above the melting point (Tsuchiya and Seymour 1985). As plotted in figure 3, at 400 °C the isotherm of the molar volume for the S–Te alloy changes almost linearly with Te composition except at the Te-rich side where the structural changes to the H form interrupt a smooth, almost linear composition dependence. After subtracting the corresponding effects in the thermodynamic mixing functions, one may find that the heat of mixing has a parabolic form with small exothermic values and the entropy of mixing is very close to the ideal mixing entropy (Maekawa *et al* 1973, Tsuchiya 1986a). Although these experimental results are rather indirect, it may be supposed that in a S–Te alloy a chain structure is preserved at low temperatures as in the Se–Te system and S and Te atoms are randomly substituted in chain molecules or parts of broken fragments from polymeric chains.

In conjunction with the electronic and thermodynamic transition in the Se–Te system, a microscopic mechanism for the structural change in chalcogen liquids has been proposed by Cutler and his co-workers (Cutler and Rasolondramanitra 1985, Cutler *et al* 1990). They have considered the behaviour of bond defects such as a D_p centre consisting of a three-fold bonded position ion, D^+, associated with a one-fold bonded negative ion, D^-, which are thermally excited in the chain molecules of neutral chalcogen atoms. Such bond defects on the one hand contribute to the paramagnetic susceptibility and to the electrical conductivity, both of which quite rapidly increase in the temperature region where the volume contracts with increasing temperature. The D_p centres in the chain, on the other hand, attract each other through electrostatic interactions, which would bring about local volume contraction and changes of atomic arrangements over a few tens of atoms around the D_p centres. Consequently it is expected that the structural change proceeds with about 10 atoms on average. This view is consistent with results independently obtained with the IHSM (Tsuchiya and Seymour 1985). Apart from the

composition and temperature dependence of the molar volume, the magnetic susceptibility (Tsuchiya 1986a) and the electrical conductivity (Kakinuma *et al* 1986) for the liquid S–Te system behave quite similarly to those for the Se–Te system. The electronic transition takes place in the temperature region where the volume contraction occurs. Since S, Se and Te all belong to the same column of the periodic table, it is very likely that the bond defects thermally excited in the S–Te chain molecules also play an essential role in the structural change, as in the Se–Te system.

4.2. Two-melt phase separation

From analysis of the mixing thermodynamic functions, the present author has estimated the interchange energy between S and Te to be about 9 kJ mol^{-1}, which contributes a small exothermic mixing enthalpy of 2.3 kJ mol^{-1} (Maekawa *et al* 1973, Tsuchiya 1986a). Since the energy associated with the ideal mixing entropy ($-TS$) for $S_{40}Te_{60}$ at 700 °C is -5.4 kJ mol^{-1}, it is difficult in the framework of a formal theory of mixture to expect the two-melt phase separation at temperatures as high as the present observation and further to explain the phase separation bounded by a closed boundary in the composition–temperature plane. In what follows we show that the rapid structural change in a Te-rich alloy causes the effective interchange energy between S and Te to be more repulsive and brings about the bounded two-melt phase separation.

To describe the structural evolution with temperature and/or pressure in the liquid Se–Te system, the present author and Seymour have developed an inhomogeneous structure model (IHSM) (Tsuchiya and Seymour 1982, 1985). The model assumes that the above-mentioned defect centre affects a group of adjacent atoms in a restricted range so as to change their local structure and such units of associated atoms form a regular mixture with remaining fragments of chain molecules. A simple Gibbs free energy has been proposed:

$$G = CG_H + (1-C)G_L + (RT/m)[C\ln C + (1-C)\ln(1-C)] + (\varepsilon_\Omega/m)C(1-C) \qquad (2)$$

where suffices H and L refer to H and L forms of mixture, respectively, and R is the gas constant. Here m is the number of atoms within a microscopic domain which cooperatively change their local structure, and each domain takes either H or L form: C is the fraction of microscopic domains in the H form. The last term represents the interaction energy between microscopic domains in different forms. Since the thermodynamic functions derived from equation (2) have been reported elsewhere (Tsuchiya and Seymour 1985), the molar volume and the thermal expansion coefficient are duplicated below for the analysis of the present results. The volume can be obtained from the relation $V = (\partial G/\partial P)_T$ together with the equilibrium condition, $(\partial G/\partial C)_{T,P} = 0$:

$$V = V_H C + V_L(1-C). \qquad (3)$$

The latter defines the temperature–pressure dependence of the fraction, C:

$$\ln C/(1-C) = -[m\,\Delta G + (1-2C)\varepsilon_\Omega]/RT \qquad (4)$$

where

$$\Delta G \equiv G_H - G_L = E_H - E_L + T(S_H - S_L) + P(V_H - V_L) = \Delta H - T\,\Delta S$$

and the symbols have their usual meanings. The thermal expansion coefficient $\alpha_P = (\partial V/\partial T)_P/V$ is readily obtained from equation (3) as

$$\alpha_P = (1/V)[CV_H\alpha_P^H + (1-C)V_L\alpha_P^L] + (1/V)(V_H - V_L)(\partial C/\partial T)_P \equiv \alpha_P^0 + \delta\alpha_P \qquad (5)$$

and

$$(\partial C/\partial T)_P = C(1-C)[m\,\Delta H + (1-2C)\varepsilon_\Omega]/\{RT^2[1-2C(1-C)\varepsilon_\Omega/RT]\}. \quad (6)$$

Stability of an alloy with respect to concentration fluctuations may be estimated from $\partial^2 G/\partial x^2$, where x is the fraction of constituents. From equation (2), we have

$$\partial^2 G/\partial x^2 = (\partial C/\partial x)(\partial\,\Delta G/\partial x) + \overline{\partial^2 G_0/\partial x^2} \quad (7)$$

where

$$\overline{\partial^2 G_0/\partial x^2} = C(\partial^2 G_H/\partial x) + (1-C)(\partial^2 G_L/\partial x^2).$$

To calculate $\overline{\partial^2 G_0/\partial x^2}$, we use a regular solution model (Wilson 1960) to a simple approximation. The first two terms of equation (2) are then written as

$$CG_H + (1-C)G_L = C[xG_{Te}^H + (1-x)G_S^H] + (1-C)[xG_{Te}^L + (1-x)G_S^L] + wx(1-x) + RT[x\ln x + (1-x)\ln(1-x)] \quad (8)$$

where the interchange energy, w, between S and Te atoms is assumed to be independent of T, P, composition and the form of an alloy. With these simplifications, we have

$$\partial^2 G/\partial x^2 = -[C(1-C)/RT](\partial m\,\Delta G/\partial x)(\partial \Delta G/\partial x)/[1-2C(1-C)\varepsilon_\Omega/RT] + [RT/x(1-x)] - 2w. \quad (9)$$

In general, the two-phase separation in a binary mixture is associated with the magnitude of $-x(1-x)\,\partial^2\Delta H_m/\partial x^2$ rather than ΔH_m in reference to the entropy term, $T\,\Delta S_m$, where ΔH_m and ΔS_m are the mixing enthalpy and mixing entropy, respectively. If the former exceeds the latter, phase separation takes place. From equation (6) we find

$$\partial^2 \Delta H_m/\partial x^2 = -[C(1-C)/RT](\partial m\,\Delta G/\partial x)(\partial \Delta G/\partial x)/[1-2C(1-C)\varepsilon_\Omega/RT] - 2w \equiv -2\omega(T). \quad (10)$$

Equation (10) indicates that the effective interchange energy, ω, becomes temperature-dependent where the structure changes with composition even if the intrinsic interchange energy, w, is independent of temperature, as we assume here. Since the first term on the right-hand side is always negative for the S–Te system, as will be shown later, $\omega(T)$ becomes more repulsive than w and the mixture becomes unstable against the concentration fluctuations.

The phase diagram has been calculated with the following assumptions. Within a microscopic region containing m atoms the composition is given by the nominal composition x and possible concentration fluctuations have been neglected. The number, m, of atoms in a microscopic domain is assumed to change linearly with the composition. In a series of papers, we have estimated the parameters for Te. It has, however, been found that the location and size of the two-melt region are very sensitive to small changes of parameters, although the two-melt region always appears in the region 30–40 at.% S and 600–800 °C. So a number of sets of values of ΔH_{Te}, ΔS_{Te} and m for Te have been tried within the previously estimated uncertainty, keeping $m\,\Delta H_{Te}$ and $m\,\Delta S_{Te}$ constant. The latter two parameters have been estimated from the V–T curve using equations (3) and (4) (Tsuchiya and Seymour 1985, Tsuchiya 1991a). Here ε_Ω was assumed to be constant and the value for Te has been used for all compositions; ΔH_S, ΔS_S and m for S have been parameterized to reproduce a two-phase region having a similar area as in the experimental results. As seen from equations (5) and (6), α_P takes

Table 2. List of parameters for structural changes in the liquid S–Te system. Where ε_Ω = 2.07 kJ and w = 8.5 kJ mol^{-1}).

	ΔH (kJ mol^{-1})	ΔS (J mol^{-1} K^{-1})	m
Te	4.320	6.822	15.73
S	4.406	0.362	5.78

a negative peaked minimum around $C = \frac{1}{2}$ for which $m\,\Delta G = \Delta G = 0$. In the present model, the position of the minimum, T^*, is given by

$$T^* = [x\,\Delta H_{Te} + (1-x)\,\Delta H_S]/[x\,\Delta S_{Te} + (1-x)\,\Delta S_S]. \tag{11}$$

Equation (11) gives a constraint on ΔH_S and ΔS_S provided that the corresponding parameters for Te are chosen. The final parameters used are listed in table 2.

Figure 8 shows temperature variation of the mixing enthalpy at several temperatures. The overall profile of ΔH_m changes quite rapidly with increasing temperature, especially on going from 300 to 400 °C. This is because the effects due to the structural change of Te to the H form mainly set in between those temperatures. At 500 °C, ΔH_m has two positive local maxima both in the Te- and S-rich sides, and a negative valley around 30 at.% S. The results are consistent with those observed experimentally (Maekawa *et al* 1973) and support the intuitive analysis previously reported (Tsuchiya 1986a). Figure 9 shows the temperature variation of $T_c = \omega(T)/Rx(1-x)$ for alloys with 30, 36, and

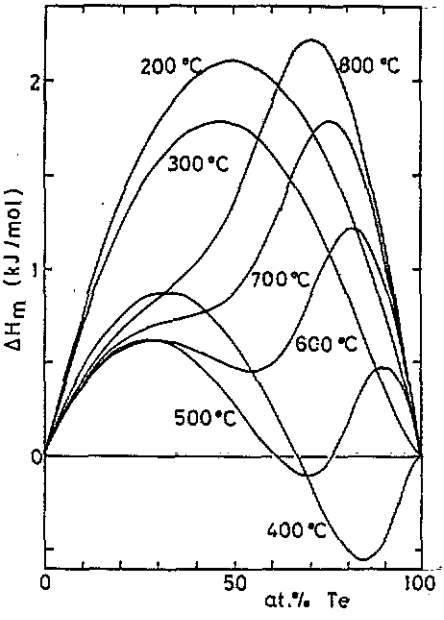

Figure 8. Calculated enthalpy, ΔH_m, for the liquid S–Te system at several temperatures.

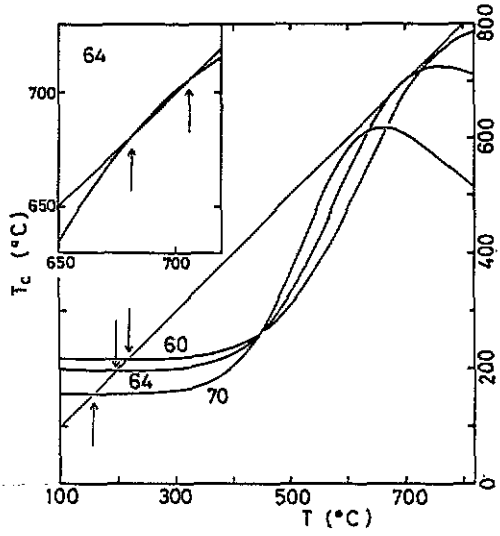

Figure 9. T_c ($=\omega(T)/Rx(1-x)$) as a function of temperature. Numbers represent atomic per cent of Te. The straight line indicates the relation $T_c = T$. The inset shows an enlarged graph for $S_{36}Te_{64}$. Arrows indicates spinodal temperatures.

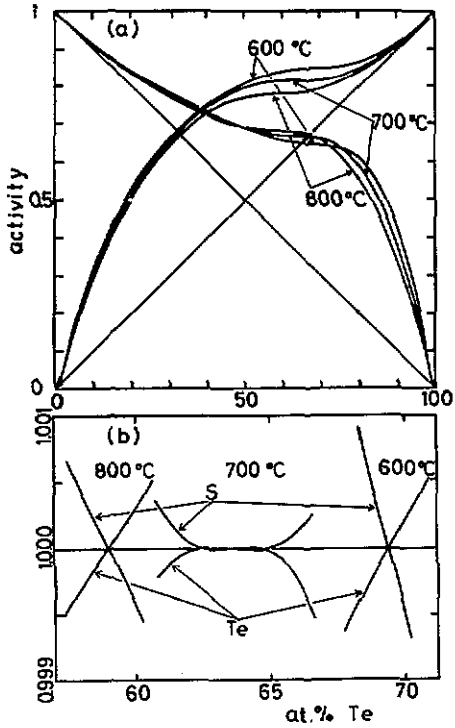

Figure 10. (*a*) Activity coefficients for S and Te as a function of Te composition at 600, 700 and 800 °C. The straight lines correspond to Raoult's law. (*b*) An enlarged graph of (*a*) near the inflection point corresponding to a maximum in the T_c–composition curve (cf figure 9) which is not apparent in the main plot. The vertical scale is expanded by a factor of about 550. Both activity coefficients are normalized to the values at the inflection points. A local minimum and a local maximum corresponding to demixing are clearly visible for the curve at 700 °C, although they are very small.

40 at.% S. T_c has a pronounced peak in the transitional region of the structural change, which mainly comes from the first term on the right-hand side of equation (10), as mentioned above, while w contributes to a constant part appearing at low temperatures. $T_c = T$ defines the spinodal line, the boundary of the region within which the one-phase system is absolutely unstable with respect to separation into two phases. As seen from figure 9, the model predicts two UCST and one LCST for $S_{36}Te_{64}$. The actual two-melt region is larger than the area within the spinodal curves, and the phase boundary (the binodal line) is determined by the condition that the respective chemical potentials for the constituents become identical on the boundary. The binodal line coincides with the spinodal line only at the critical points. In figure 10, the activity coefficients for Te and S are plotted at several temperatures, from which the two-melt boundary has been graphically determined. As inferred from the enlarged graphs in figures 9 and 10, the phase separation around 700 °C results from a very delicate balance of energies between those associated with the structural transition and the mixing entropy. The theoretical phase diagrams have been compared with the experimental results in figures 6 and 7. Bearing in mind the very simple model used, IHSM can satisfactorily reproduce the essential features of the phase diagram. The model also predicts a phase separation having upper critical temperature 238 °C ($=w/2R$) and 50 at.% S, which would occur well below the equilibrium liquidus line as plotted in figure 7 and therefore not be observed.

It would be of interest to see the effects on phase separation of an applied pressure. Calculation is rather straightforward in the low-pressure region because the effects of an applied pressure enter mainly through the pressure dependence of the parameter C which is brought about by a $Pm\ \Delta V$ term in $m\ \Delta G$ of equation (4) and all other parameters

can be assumed to be pressure-independent to a rough approximation. From the V–T curve in figure 2, we find that the volume contraction ΔV associated with the structural change is about $-3\ \mathrm{cm^3\ mol^{-1}}$, which amounts to reduction of ΔH by $300\ \mathrm{J\ mol^{-1}}$ upon an applied pressure of 1×10^8 Pa (=1 kbar). All other parameters were kept constant, as listed in table 2. Although the results are rather qualitative, the model predicts that an applied pressure significantly enlarges the two-phase region as plotted in figure 7. The reason is that an applied pressure stabilizes the high-temperature form of a S–Te alloy because of its smaller volume and moves the transitional region of the structural change to lower temperatures. Consequently, an applied pressure effectively increases the enthalpy term with respect to the entropy term. Roughly speaking, the peak of T_c in figure 9 shifts to lower temperatures with an applied pressure while keeping its peak value almost constant, and then an alloy becomes unstable against the concentration fluctuations in a much wider range of composition and temperature.

As shown previously, the structural change in the liquid Se–Te system (Tsuchiya 1986b) is much the same and the first term on the right-hand side of equation (7) becomes of the same order of magnitude as that for the S–Te system. This means that a tendency for segregation develops in the temperature–composition plane where the thermodynamic parameters have extrema. The high-resolution radial distribution function of $Se_{25}Te_{75}$ (Misawa and Suzuki 1980) has provided unexplained results, namely that unlike-atom correlation becomes weakened and the probability of the formation of Se–Se and Te–Te like-pairs increases in the transitional temperature region of structural changes. The present calculation, however, shows that phase separation in the liquid Se–Te system would not take place because the interchange energy between Se and Te atoms is negative and cancellation occurs in the terms associated with the structural change and the interchange energy.

5. Conclusions

The molar volume of the liquid S–Te system as a function of temperature and composition has been investigated by the high-energy γ-ray attenuation method. The results indicate that the S–Te system undergoes rapid structural changes as does the Se–Te system. The bounded two-melt region has been found in the course of the investigation. It is located well above the equilibrium liquidus line where the non-metal–metal transition takes place. The appearance of the lower critical solution temperature (LCST) and the upper critical solution temperature (UCST) in a liquid S–Te alloy is a consequence of rapid structural change in the liquid. The inhomogeneous structure model (IHSM) satisfactorily explains the essential features of the phase equilibria of the liquid S–Te system.

References

Cutler M and Rasolondramanitra H 1985 *Localization and Metal–Insulator Transitions* ed H Fritzsche and D Adler (New York: Plenum) p 119

Cutler M, Kao S S and Silva L 1990 *Phys. Rev.* B **41** 3339

Hansen M and Anderko K 1958 *Constitution of Binary Alloys* 2nd edn (New York: McGraw-Hill) p 1165

Kakinuma F and Ohno S 1987 *J. Phys. Soc. Japan* **56** 619

—— 1988 *Z. Phys. Chem., NF* **156** 265

Kakinuma F, Okada T and Ohno S 1986 *J. Phys. Soc. Japan* **55** 284

Kellas A M 1918 *J. Chem. Soc.* **113** 903
Maekawa T, Yokokowa T and Niwa K 1973 *Bull. Chem. Soc. Japan* **46** 761
Mennele A, Bellissent R and Flank A M 1988 *Europhys. Lett.* **4** 707
—— 1989 *Physica* B **156 & 157** 174
Misawa M and Suzuki K 1980 *J. Physique Coll.* C8 203
Takimoto K and Endo H 1982 *Phys. Chem. Liq.* **12** 141
Thurn H and Ruska J 1976 *J. Non-Cryst. Solids* **35 & 36** 1263
Tobolsky A V and MacKnight W J 1965 *Polymeric Sulfur and Related Polymers* (New York: Interscience)
Tsuchiya Y 1986a *J. Phys. C: Solid State Phys.* **19** 2865
—— 1986b *J. Phys. C: Solid State Phys.* **19** 1389
—— 1988 *J. Phys. Soc. Japan* **57** 3851
—— *1989 J. Non-Cryst. Solids* **117/118** 571
—— 1991a *J. Phys.: Condens. Matter* **3** 3163
—— 1991b *J. Phys. Soc. Japan* **60** 960
Tsuchiya Y and Seymour E F W 1982 *J. Phys. C: Solid State Phys.* **15** L687
—— 1985 *J. Phys. C: Solid State Phys.* **18** 4721
Wilson A H 1960 *Thermodynamics and Statistical Mechanics* (Cambridge: Cambridge University Press) 420
Winter R, Szornel C, Pilgrim W-C, Howells W S, Egelstaff P A and Bondensteiner T 1990 *J. Phys.: Condens. Matter* **2** 8424